NJC

Accepted Manuscript

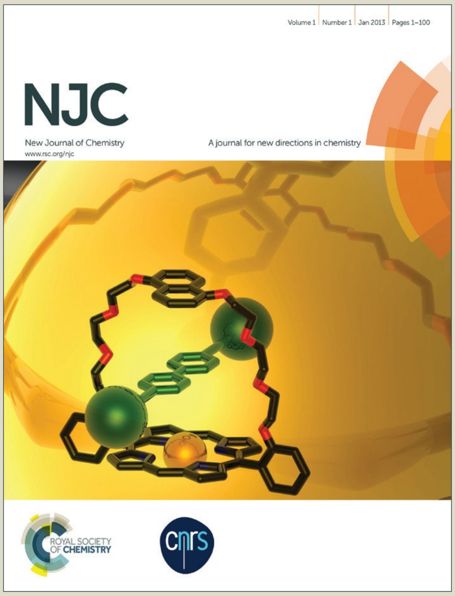

ROYAL SOCIETY OF CHEMISTRY

www.rsc.org/njc

Journal Name

ARTICLE

Received 00th January 20xx,
Accepted 00th January 20xx

DOI: 10.1039/x0xx00000x

www.rsc.org/

A Novel Redox Responsive Chiral Cyclometalated Platinum(II) Complexes with Pinene Functionalized C^N^N Ligands

Xiao-Peng Zhang,[ab] Fu-Qiang Liu,*[a] Jian-Cheng Lai,[b] Cheng-Hui Li,*[b] Ai-Min Li[a] and Xiao-Zeng You[b]

By oxidation of a couple of chiral cyclometalated platinum(II) complexes**,** Pt(L_a)(C≡C−Ph) (**1a**) and Pt(L_b)(C≡C−Ph) (**1b**) (L_a = (-)-4,5-pinene-6'-phenyl-2,2'-bipyridine, L_b = (+)-4,5-pinene-6'-phenyl-2,2'-bipyridine), a novel pair of platinum(IV) enantiomers, Pt(L_a)(C≡C−Ph)$_3$ (**2a**) and Pt(L_b)(C≡C−Ph)$_3$ (**2b**), were obtained. According to single crystal X-ray diffraction studies of **2a** and **2b**, the central platinum atom is wrapped by a C^N^N ligand and three phenylacetylene groups and exhibits a distorted octahedral geometry. Due to the different coordination configurations and electronic structures, complexes **2a** and **2b** are distinct from **1a** and **1b** not only in absorption and emission spectra, but also in their chiroptical properties. The oxidation reaction of **1a** and **1b** is a kinetically controllable process. Given different oxidants to complete the Pt(II)-to-Pt(IV) process, various oxidation rates were presented. The difference in ECD spectrum between complexes **1a** and **2a** has been confirmed through TD-DFT calculation and can be useful for designing new redox-responsive materials.

1. Introduction

Redox-responsive chiral materials have been proven to play considerable roles in various high-technology fields, such as optical displays, chiral electrodes, information storage, stereoselective catalysis and biological systems.[1-4] Through oxidation or reduction chemically or electrochemically, chiral compounds can form two or more stable oxidation states with different configurations or variable packing structures.[5-8] Furthermore, the redox processes can be highly selective and fast. During these processes, significantly different absorptions, emission spectroscopies, circular dichroism signals or other interesting chiroptical properties can be observed. Therefore, more information about molecular conformation or intermolecular association can be obtained in the structure-transformation process, and further application regarding redox-responsive materials may be explored.[9,10]

Planar platinum(II) complexes are sensitive to various external stimuli, such as volatile vapor exposure,[11-14] mechanical force,[15-18] reducing/oxidizing agents[19] and temperature[20-22], accompanying with changes of intriguing chemical and physical properties in these stimuli-responsive processes. Such kind of switches are useful for a wide variety of applications, including optical recording, memory, sensing, display and catalysis.[23-25] The oxidation of platinum(II) complexes can be facilely conducted with oxygen, hydrogen peroxide, halogen and other oxidants,[26-29] while the UV-Vis absorptions, emissions, and chiroptical properties of Pt(IV) complexes would be quite different from those of Pt(II) complexes due to distinct coordination conformations and electronic structures. Therefore, they can be used in chiral probes or electrodes. However, few reports have been devoted to chiral platinum complexes.[30,31]

We have previously studied the stimuli-induced transformation (e.g. vapor, mechanical force) of a series of chiral cyclometalated platinum(II) complexes both in solution and solid state by electronic circular dichroism (ECD), vibrational circular dichroism (VCD), and circular polarized luminescence (CPL).[32-34] Of particular interest is the chiral platinum(II) complexes with pinene functionalized C^N^N ligands, showing interesting vapor-induced chiroptical switching properties.[35]

According to previous studies, when pinene groups are introduced, the steric hindrance is increased and molecules become more rigid. Therefore, the intermolecular aggregations (Pt···Pt and $\pi-\pi$ contacts) would be hampered and the self-quenching of platinum(II) complexes may be effectively prevented.[36,37] Additionally, by incorporation of bulky and chiral pinene groups, the planarity of platinum(II) complexes could be reasonably distorted or the adjacent molecules could be staggered from each other alongside the Pt···Pt chain, resulting in metal center chirality or helical packing environment, which may give rise to interesting chiroptical properties.[38,39] More importantly, the electronic structure and energy band gap may be changed when pinene groups are incorporated, therewith an extraordinary redox characteristic would be presented.

In this work, by oxidation of a couple of pinene-containing chiral cyclometalated platinum(II) complexes, Pt(L_a)(C≡C−Ph) (**1a**) and Pt(L_b)(C≡C−Ph) (**1b**) (L_a = (-)-4,5-pinene-6'-phenyl-2,2'-bipyridine, L_b = (+)-4,5-pinene-6'-phenyl-2,2'-bipyridine), one couple of novel

---

[a] State Key Laboratory of Pollution Control and Resource Reuse, School of the Environment, Nanjing University, Nanjing 210046, People's Republic of China,E-mail:jogia@163.com;Fax: +86-25-89680377; Tel: *+86-25-89680377*

[b] *State Key laboratory of Coordination Chemistry, School of Chemistry and Chemical Engineering, Collaborative Innovation Center of Advanced Microstructures, Nanjing university, Nanjing 210093, People's Republic of China, E-mail:* chli@nju.edu.cn

† CCDC 1401347 (**2a**) and 1401348 (**2b**). Electronic Supplementary Information (ESI) available. See DOI: 10.1039/x0xx00000x

enantiomeric cyclometalated platinum(IV) complexes Pt(L_a)(C≡C−Ph) (**2a**) and Pt(L_b)(C≡C−Ph) (**2b**) were isolated (Chart 1). These two oxidation forms Pt(II)/(IV) are very stable in solution and solid state at room temperature. Due to the different coordination configurations and electronic structures, complexes **2a** and **2b** are distinct from **1a** and **1b** not only in absorption and emission spectra, but also in their chiroptical properties. The oxidation reaction of **1a** and **1b** is a kinetically controllable process. Upon addition with 5 equivalents hydrogen peroxide or other common oxidants, **1a** and **1b** could undergo oxidation in solution quickly in several seconds or sluggishly in two days. The color changed from yellow to colorless in the oxidation process, meanwhile the luminescence faded away and the ECD spectrum differed significantly. The difference in ECD spectrum between complexes **1a** and **2a** has been confirmed through TD-DFT calculation and can be useful for designing new redox-responsive materials.

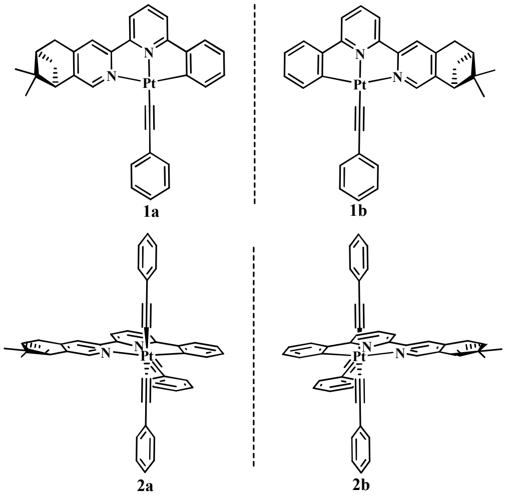

Chart 1. Molecular structures of **1a**, **1b**, **2a** and **2b**.

2. Experimental Section

2.1 General Methods

All reagents were purchased from commercial suppliers and used as received. Mass spectra were acquired on Time of Flight Mass Spectrometer. ^{1}H-NMR spectra were obtained on a DRX 500 NMR spectrometer. Chemical shifts are referenced to TMS. Coupling constants are given in hertzs. UV-Vis spectra were measured on a UV-3600 spectrophotometer. The ECD spectra were recorded on a Jasco J-810 spectropolarimeter by using 1 cm quartz cell. The X-ray photoelectron spectroscopy (XPS) were carried out by a PHI 5000 VersaProbe (U1VAC-PHI), and binding energies were measured relative to the C 1s peak (284.8 eV) of internal hydrocarbon. Cyclic voltammetry was recorded on an IM6ex electrochemical workstation at room temperature and under argon, with platinum as the working and counter electrodes, Ag/AgCl in saturated KCl (aq) as the reference electrode, and 0.1 M n-Bu_4NClO_4 as the supporting electrolyte. The scanning rate was 100 mV/s. Potential is reported in V vs $Cp_2Fe^{+/0}$

2.2 Synthesis

The precursors **1a** or **1b** were prepared according to our previously reported methods.[35] The chiral platinum(II) complexes **2a** or **2b** were obtained according to Scheme 1. In the absence of light, **1a** (1 mmol), phenylacetylene (5 mmol), Et_3N (5 mmol) and CuI (20 mg) were stirred in an anhydrous dichloromethane solution without protection of argon atmosphere. After reacting at room temperature for 24 h, the solvent was evaporated in vacuo. The pale yellow powders were obtained by chromatography on a silica gel column using PE : EA = 1 : 1. Yield: 85%. Moreover, in argon atmosphere, complexes **2a** or **2b** also can be obtained by the oxidation of **1a** and **1b** with benzoyl peroxide (5 mmol) at the same reaction condition (identical amounts of phenylacetylene, NEt3 and CuI, as above). MS (ESI) (m/z): $[M]^+$ calcd for $C_{47}H_{36}N_2Pt$, 823.2; found, 823.1. ^{1}H NMR (500 MHz, DMSO-d6): δ 8.77 (s, 1H, Py), 8.68 (s, 1H, Py), 8.55 (d, J = 7.5Hz, 1H, Py), 8.44 (t, J = 8.0Hz, 1H, Py), 8.41 (t, J = 8.0Hz, 1H, Py), 7.99-8.03 (m, 2H, Ph), 7.58 (d, J = 7.5Hz, 2H, Ph), 7.38 (t, J = 8.0Hz, 1H, Ph), 7.35 (t, J = 7.5Hz, 2H, Ph), 7.30 (t, J = 7.5Hz, 1H, Ph), 7.24 (t, J = 7.5Hz, 1H, Ph), 7.03 (t, J = 6.5Hz, 2H, Ph), 6.98-7.02 (m, 4H, Ph), 6.76 (d, J = 7.0Hz, 2H, Ph), 6.71 (d, J = 7.0Hz, 2H, Ph), 3.27-3.31 (m, 2H, CH_2), 3.24 (m, 1H, CH_a), 2.75-2.79 (m, 1H, CH), 2.35 (m, 1H, CH), 1.43 (s, 3H, CH_3), 1.25 (d, J = 9.5Hz, 1H, CH_b), 0.65 (s, 3H, CH_3).

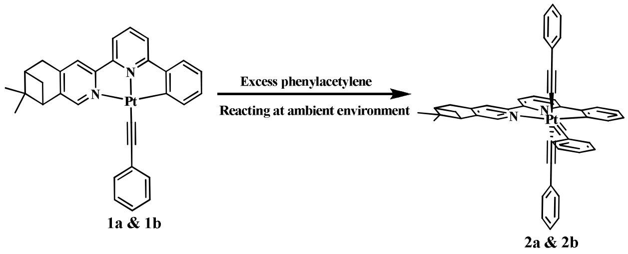

Scheme 1. Synthetic routes of **2a** and **2b**.

2.3 X-ray structure determination

Single-crystal X-ray diffraction measurements were carried out on a Bruker SMART APEX CCD based on diffractometer operating at room temperature. Intensities were collected with graphite monochromatized Mo Kα radiation (λ = 0.71073 Å) operating at 50 kV and 30 mA, using $\omega/2\vartheta$ scan mode. The data reduction was made with the Bruker SAINT package.[40] Absorption corrections were performed using the SADABSprogram.[41] The structures were solved by direct methods and refined on F^2 by full-matrix least-squares using SHELXL-2014 with anisotropic displacement parameters for all non-hydrogen atoms in all two structures. Hydrogen atoms bonded to the carbon atoms were placed in calculated positions and refined as riding mode, with C–H = 0.93 Å (methane) or 0.96 Å (methyl) and Uiso(H) = 1.2Ueq ($C_{methane}$) or Uiso(H) = 1.5Ueq (C_{methyl}). The water hydrogen atoms were located in the difference Fourier maps and refined with an O-H distance restraint [0.85(1) Å] and Uiso(H) = 1.5 Ueq(O). All computations were carried out using the SHELXTL-2014 program package.[42]

2.4 Computational details

The calculations were carried out by density functional theory (DFT) method at B3LYP level with Gaussian03 program.[43] The crystal structures were used as the starting geometries. The geometries of **1a** and **2a** were fully optimized without any symmetry constraints. The excitation energies were calculated by time-dependent density functional theory (TD-DFT) and 50 excited electronic states were considered. The effect of the solvent was modeled by the CPCM dielectric model with acetonitrile solution. The 18-valence electron Stuttgart small core relativistic pseudo-potentials with their corresponding optimized set of basis functions were employed for the Pt atom,[44] while the standard split-valence 6–31G* basis set for were used for all other atoms.

3. Results and discussion

3.1 Crystal structures

Single crystals **2a** and **2b** (pale yellow blocks) suitable for X-ray measurement were obtained by slow evaporation of acetonitrile/acetone (v/v = 3:1) and acetonitrile/acetone (v/v = 1:1) solution, respectively. Complexes **2a** and **2b** crystallize in the same chiral space group, $P2_12_12_1$ of the orthorhombic system (Table 1), with one complex molecule per asymmetrical region. Although complex **2a** contains an additional co-crystallized acetonitrile molecule in the crystal lattice compared to **2b** and shows a corresponding larger lattice volume than that of complex **2b** (Table 1), their structures are almost mirror-symmetric (Fig. 1).

Table 1. Crystallographic data of compounds **2a** and **2b**.

	2a•CH$_3$CN	**2b**
Formula	$C_{49}H_{39}N_3Pt$	$C_{47}H_{36}N_2Pt$
Mr/g mol^{-1}	864.92	823.87
crystal system	orthorhombic	orthorhombic
Space group	$P2_12_12_1$	$P2_12_12_1$
a/Å	11.2437(5)	14.7779(6)
b/Å	15.0330(8)	14.8743(6)
c/Å	23.3412(11)	16.8574(7)
α/ °	90.00	90.00
β/ °	90.00	90.00
γ/ °	90.00	90.00
V/Å^3	3945.3(3)	3705.4(3)
Z	4	4
T /K	296(2)	296(2)
Radiation, λ /Å	0.71073	0.71073
D_{calcd}, g/cm^{-3}	1.456	1.477
μ/mm^{-1}	3.594	3.822
F(000)	1728	1640
Crystal size/mm^3	0.29×0.24×0.20	0.32×0.28×0.20
ϑ range/°	1.61 to 27.52	1.83 to 27.55
Reflections measured	26915	25151
Unique reflections	9034	8540
R_{int}	0.0260	0.0292
Reflections withF^2>2σ(F^2)	8436	7751
Number of parameters	481	453
Goodness-of-fit on F^2	1.026	1.001
R_1 [F^2> 2σ(F^2)]	0.0219	0.0255
wR_2 (all data)	0.0496	0.0621
$\Delta\rho_{max,}\Delta\rho_{min}$ /e Å^{-3}	0.827, -0.602	0.900, -0.449
Flack parameter	0.005(4)	-0.022(4)
refine_ls_shift/su_max	0.002	0.000
refine_ls_shift/su_mean	0.000	0.000

In the crystal structures of complexes **2a** and **2b**, one carbon atom and two pyridyl nitrogen atoms of the C^N^N ligand, and three acetenyl carbon atoms coordinate to the platinum nucleus, which exhibits a distorted octahedral geometry. (Fig. 1). For both complexes **2a** and **2b,** Pt−C and Pt−N bond distances as well as corresponding chelating bite angles resemble those octahedral Pt(IV) complexes reported before.[29, 45-48] Selected bond lengths and angles are summarized in Table 2. The bond lengths of Pt−C and Pt−N reside in the range of 1.980(4) to 2.111(5) Å, and 2.013(4) to 2.174(3) Å, respectively. However, due to the presence of an acetonitrile molecule in **2a**, some difference are exhibited for Pt1-C3 and Pt1-C4 bond distances of **2a** and **2b**.[34,39] Around the platinum nucleus, the bite angels C2−Pt1−C4 (179.18(14)° in **2a** and 176.27(15)° in **2b**) and C3−Pt1−N2 (178.65(13)° in **2a** and 178.73(16)° in **2b**) are close to 180°. Nonetheless, owing to the strain effect of chelating metallacycles, the C1−Pt1−N1 angle (159.57(13)° in **2a** and 159.43(15)° in **2b**) deviates significantly from a linar geometry, and this deviation results in a distorted octahedral geometry of Pt(IV) center. Moreover, as the coordination environment changes from a square planar for **1a** to an octahedral geometry for **2a**, Pt−C and Pt−N distances become longer (Table 2), which is characteristic for Pt(IV) complexes.[46] The equatorial ring of phenylacetylene is almost coplanar with the Pt(C^N^N) unit with torsion angles being 166.73° in **2a** and 170.08° in **2b,** while the dihedral angle between the axial phenylacetylene ligands is 133.13° and 133.52° for **2a** and **2b**, respectively.

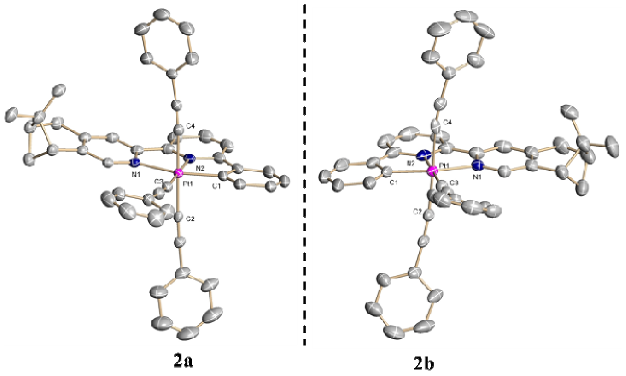

Fig. 1. X-ray crystal structures of **2a** and **2b**. H atoms and solvent molecules are omitted for clarity.

Table 2. Structural parameters of complexes **2a** and **2b**determined by X-ray single crystal diffraction.

Bond	**2a**	**2b**	Bond	**2a**	**2b**
Pt1−C1	2.016(4)	2.021(4)	C1−Pt1−C2	88.35(13)	85.12(17)
Pt1−C2	2.045(3)	2.037(4)	C1−Pt1−C3	98.60(16)	97.58(17)
Pt1−C3	1.980(4)	2.038(4)	C1−Pt1−C4	91.32(14)	92.95(16)
Pt1−C4	2.036(4)	2.111(5)	C1−Pt1−N1	159.57(13)	159.43(15)
Pt1−N1	2.169(3)	2.174(3)	C1−Pt1−N2	81.58(15)	82.52(17)
Pt1−N2	2.015(3)	2.013(4)	C2−Pt1−C3	90.10(13)	89.64(16)
			C2−Pt1−C4	179.18(14)	176.27(15)
			C2−Pt1−N1	94.71(11)	93.80(14)
			C2−Pt1−N2	91.25(12)	91.63(15)
			C3−Pt1−C4	89.22(14)	87.45(14)
			C3−Pt1−N1	101.58(13)	102.96(14)
			C3−Pt1−N2	178.65(13)	178.73(16)
			C4−Pt1−N1	85.86(13)	89.12(13)
			C4−Pt1−N2	89.44(13)	91.28(13)
			N1−Pt1−N2	78.17(12)	76.97(14)

Crystal packing diagrams of **2a** and **2b** are presented in Fig. 2. Due to the steric hindrance of bulky ligands, the absence of Pt-Pt interactions can be expected. As viewed along *b*-axis, two molecules of **2a** are packed side by side in the *a*-axis with effective π–π interactions connecting them. Similarly, complex **2b** employs a side by side arrangement along the *a*-axis, however, the intermolecular π–π interaction is weakened due to less compacted packing. Moreover, different inclined degrees (the angle between the connecting line C2-C4 of axial phenylacetylene ligands and the *a*-axis) of single molecule in the *ac* plane are exhibited in **2a** and **2b** (23.922° in **2a** and 16.759° in **2b**), suggesting that the insertion of co-crystallized solvent molecule into the crystal lattice has a moderate effect on the molecule packing.

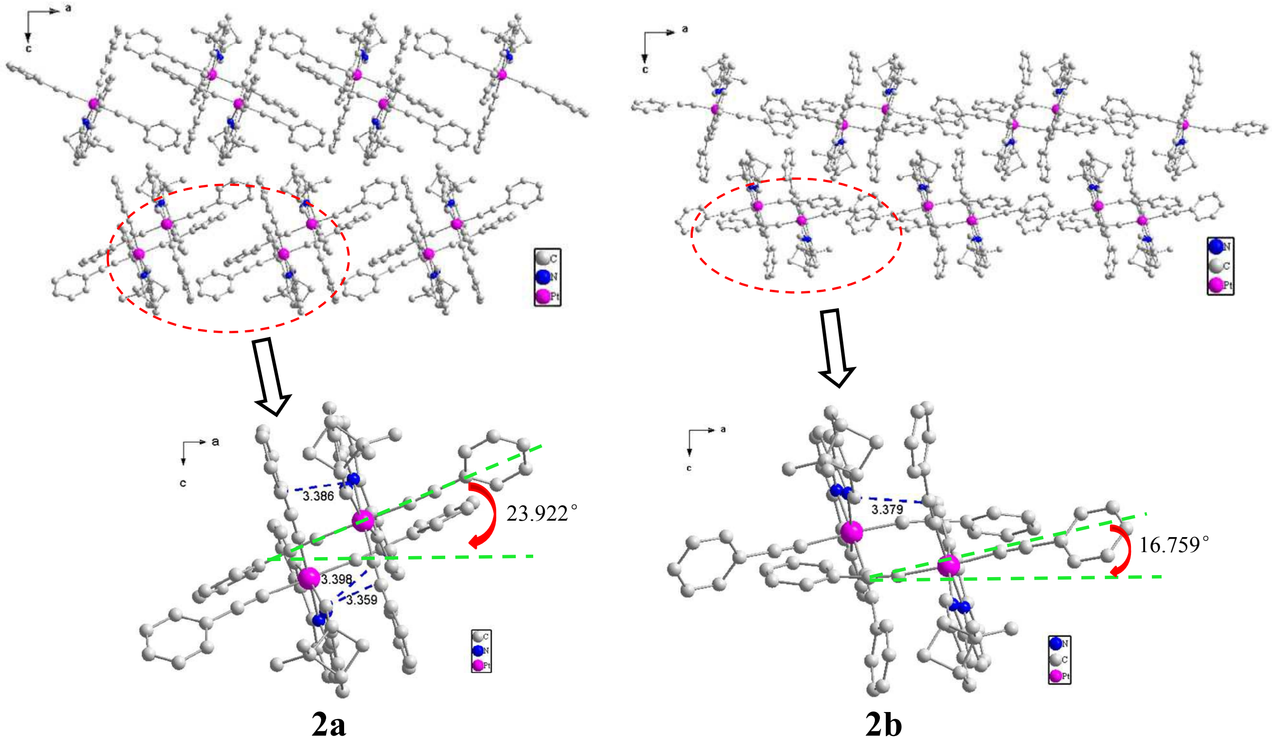

Fig. 2. Crystal packing diagrams of **2a** and **2b** viewed along *b*-axis with blue dashed lines indicating the π–π interaction.

3.2 UV-Vis Absorption and Electronic Circular Dichroism Spectra (ECD)

The UV-Vis and ECD spectra of the enantiomeric platinum(II)/(IV) coordination complexes in acetonitrile solution are shown in Fig. 3, The UV-Vis spectra of enantiomers are identical while the ECD spectra are almost mirror-symmetric to each other. We therefore only describe those of **1a** and **2a**. Complex **1a** exhibits characteristic transitions of aromatic chromophores in the band of 200-370 nm. This series of intense transitions with ε exceeding 10^4 L·mol^{-1}·cm^{-1} are ascribed to intraligand (IL) charge-transfer transitions. A broad peak centering in the region of 380-500 nm ($\varepsilon > 10^3$ L·mol^{-1}·cm^{-1}) are attributed to ^{1}MLCT (metal-to-ligand charge transfer) mixed with ^{1}LLCT (ligand-to-ligand charge transfer) transitions.[49-53]

Owing to different coordination configurations and higher oxidation states of Pt nucleus, the absorption spectrum of complex **2a** is markedly different from **1a**. For complex **2a**, a very strong peak at 250 nm ($\varepsilon > 5 \times 10^4$L·mol^{-1}·cm^{-1}) along with a band of poorly resolved transitions locating at 300-380 nm were displayed, which can be assigned as intraligand (IL) charge-transfer and ^{1}LLCT transitions, respectively. Because Pt(IV) is the high valence state, low-energy MLCT transitions can't be occurred, and almost no transition bands above 400 nm have been found.[46]

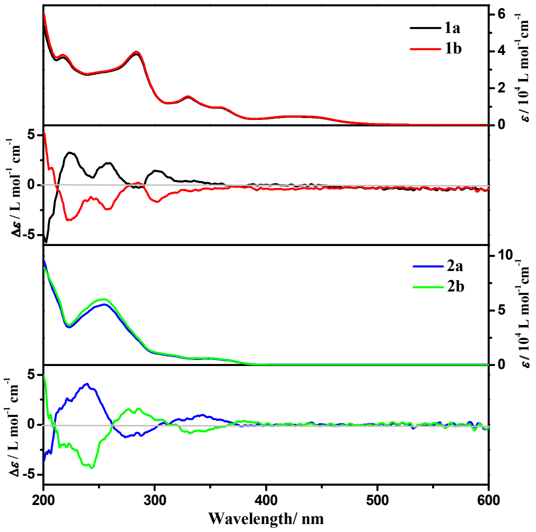

Fig. 3. UV-vis and ECD spectra of enantiomers **1a** and **1b** (3.75×10^{-5}mol·L^{-1}), **2a** and **2b** (2.5×10^{-5}mol·L^{-1}) in acetonitrile solution.

The difference in absorptions of complexes **1a** and **2a** is ascribed to different electronic structures, as evidenced by the difference in their highest occupied molecular orbital (HOMO) and lowest unoccupied molecular orbital (LUMO) (Fig. 4). The LUMO of both **1a** and **2a** is located on the two pyridine rings of C^N^N moiety with a small contribution of the platinum atom. However, the HOMO of **1a** is mainly located on the platinum atom and phenylacetylenefragment,[54] while the HOMO of **2a** is mainly located on the two axial phenylacetyleneligands.[55] Therefore, the low energy MLCT transition is present in **1a** but not in **2a**. Furthermore, the difference of low-energy transition is revealed by the TD-DFT calculation. The simulated UV-Vis spectrum of **1a** tails down to 480 nm, while that of **2a** only extends to 390 nm (Fig. 5).

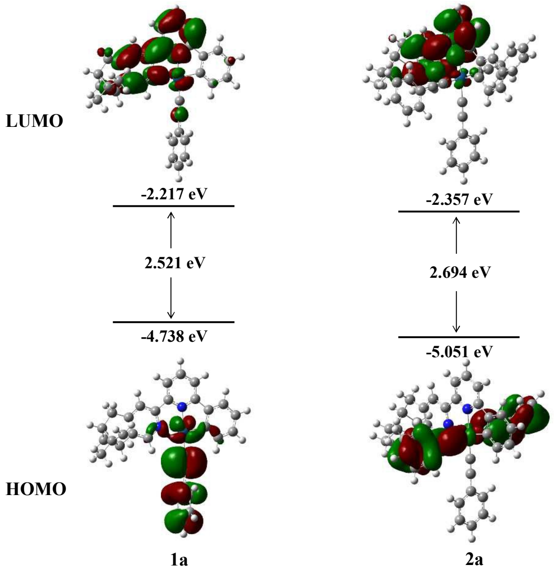

Fig. 4. Contour plots of the HOMOs and LUMOs of **1a** and **2a**.

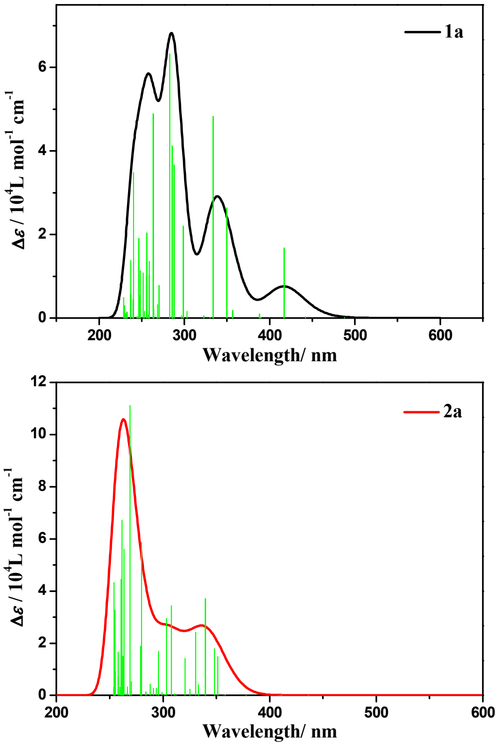

Fig. 5. Computed UV-Vis spectra of complex **1a** and **2a** in acetonitrile solution. The green column is the computed rotatory strength

As shown in the Fig. 3, the ECD spectrum of complex **1a** shows positive Cotton effects at 224 nm, 258 nm and 302 nm, with a weak negative Cotton effects at 285 nm. However, two positive Cotton effects (241 nm and 344 nm) as well as one negative Cotton effect at 280 nm are observed for complex **2a**. In comparison with absorption spectra, some distinguishable positive Cotton effects originating form MLCT are presented at ca. 420 nm and tail down to 480 nm for complex **1a**, while no Cotton effects are observed above 400 nm for complex **2a**. Herein, it can be tentatively presumed that a change of configuration, resulting from a diversification of oxidation state of central platinum ion, would have a significant influence on the chiral environment.[30] The ECD spectra **1a** and **2a** are mirror images of their enantiomers. The simulated ECD spectra from TD-DFT calculations of **1a** and **2a** are in good agreement with the experimental results with regard to the shape (Fig. 6 and Fig. 7).

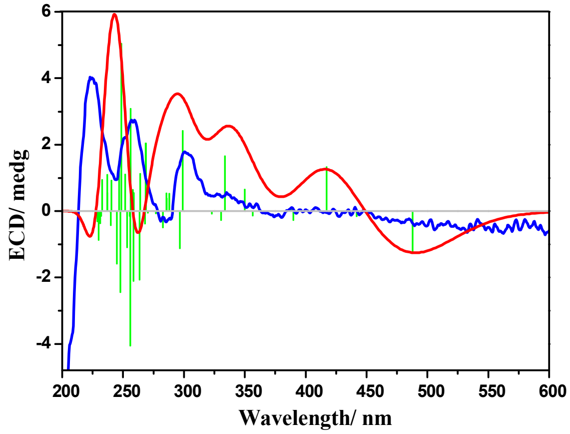

Fig. 6.Computed ECD spectra of complex **1a** in acetonitrile solution (red) compared to experiment (blue). The green column is the computed rotatory strength.

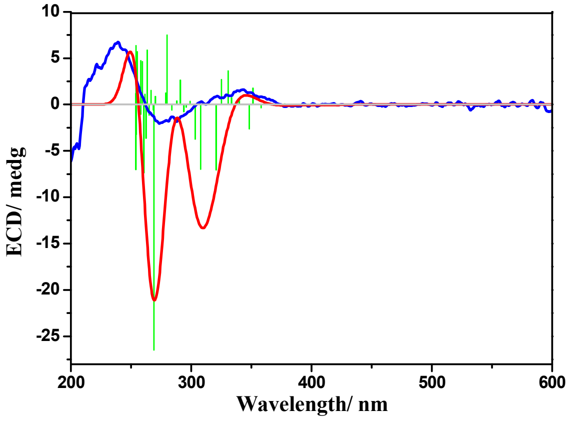

Fig. 7. Computed ECD spectra of complex **2a** in acetonitrile solution (red) compared to experiment (blue). The green column is the computed rotatory strength.

3.3 Redox-induced Chiroptical Variation

In the presence of oxygen, unprecedented Pt(IV) complexes **2a** and **2b** can be obtained by reaction platinum(II) complexes **1a** and **1b** with excess phenylacetylene. However, the oxidation reaction did not occur in the absence of oxygen. We tentatively assume that the Pt(II)-to-Pt(IV) transformation only can proceed with the help of oxidants. Thereupon, several common oxidants (30% hydrogen peroxide water solution, 85% sodium hypochlorite water solution, sodium persulfate and benzoyl peroxide) were selected to perform the oxidations of **1a** and **1b**. It is noteworthy that, when excess different oxidants (5 equivalents) were used, complexes **1a** and **1b** could be oxidized quickly or slowly. The complete oxidations of **1a** and **1b** need several seconds for sodium hypochlorite, 30 minutes for hydrogen peroxide, 2 hours for sodium persulfate, and two days for benzoyl peroxide. Accordingly, the oxidation can be considered as a kinetically controllable process.[26] After the oxidation, the color of solution changed from yellow to colorless, and the luminescence vanished (Fig. 8).

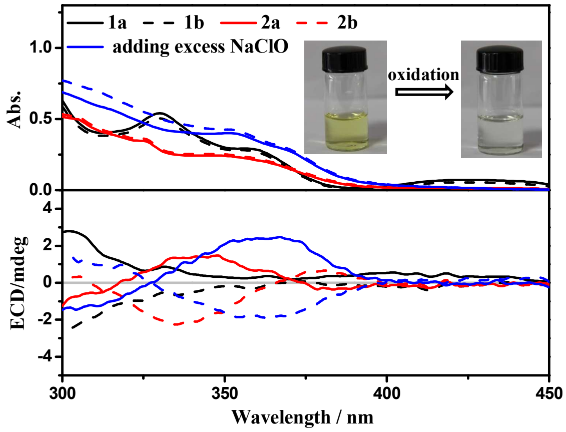

Fig. 8. UV-Vis and ECD spectra of complexes **1a** and **1b**, **2a** and **2b**, **1a** and **1b** after addition excess NaClO.

To determine oxidation states of Pt ions, XPS measurements were carried out. As shown in Fig. 9, complex **1a** exhibits the Pt $4f_{5/2}$ and $4f_{7/2}$ binding energies of 76.3 and 72.9 eV, respectively, typical characters of Pt(II) species.[56-57] The Pt $4f_{5/2}$ and $4f_{7/2}$ binding energies for **2a** are determined to be 78.5 and 75.4 eV, respectively, which agree well with the values of reported Pt(IV) complexes.[58-59] The chemical state of the oxidation product of sodium hypochlorite also has been examined, and Pt $4f_{5/2}$ and $4f_{7/2}$ binding energies, centered at 78.4 and 75.3 eV, respectively, are unambiguously observed, further confirming the formation of Pt(IV) compounds in the oxidation processes. In addition, the peaks resided at 76.3 and 72.9 eV can not be detected in the oxidation product of sodium hypochlorite, and it could be inferred that all most of Pt(II) complexes has been transformed into Pt(IV) ones.

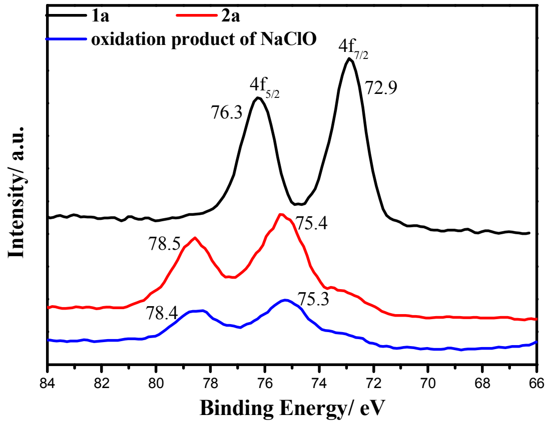

Fig. 9. Pt $4f_{5/2}$ and $4f_{7/2}$ core levels of XPS for **1a**, **2a** and the oxidation product of sodium hypochlorite.

Despite different oxidants used, the UV-Vis and ECD spectra (300-450 nm) of oxidation products are similar with complexes **2a** and **2b** (Fig. 8 and Fig. 10). In the ECD spectra, complexes **1a** and **1b** show a weak absorption at ca. 430 nm and a weak peak can be observed in the range 400 nm to 450 nm. However, a moderate peak centering 340-380 nm is presented for Pt(IV) complexes, which is absent in Pt(II) complexes. Therefore, this band at 340-380 nm can be served as a diagnostic peak to distinguish Pt(II) and Pt(IV) complexes, also can be used to monitor redox reaction of chiral cyclometalated Pt(II) complexes. Mostly, The luminescent and chiroptical properties of square-planar Pt(II) complexes can be reversibly switched by means of various external stimuli,[20, 60-63] such as temperature, solvents, ultrasound, acid/base and so on. The tuning of optical activity was frequently facilitated by variations of conformation or intermolecular packing. The center platinum atom remained in a low valence state Pt(II) during these process. In the present study, the valence state of metal nucleus was transformed from Pt(II) to Pt(IV), correspondingly the coordination geometry, electronic structure and optical performance have changed. The Pt(IV) complexes resulting from oxidation of **1a** have been tried to be reversed to the original Pt(II) state by different reducing agents (ascorbic acid, triphenylphosphine and sodium hydride).[64] Unfortunately, the reductions seems to be unsuccessful and no changes of color, luminescence and ECD have been observed after three days.

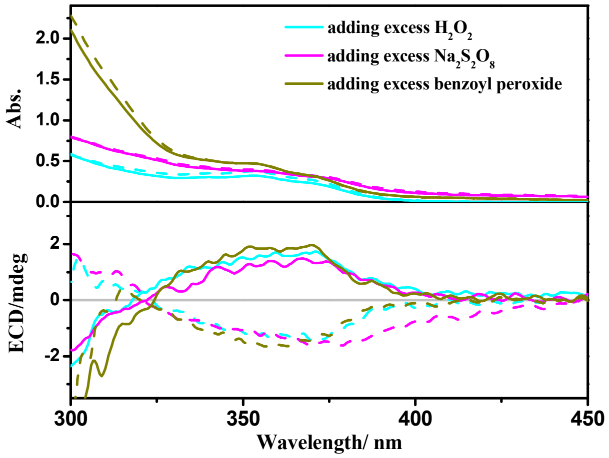

Fig. 10. UV-Vis and ECD spectra of complexes **1a** and **1b** after addition excess H_2O_2, $Na_2S_2O_8$ and benzoyl peroxide.

Cyclic voltammetry was performed on complex **1a** at room temperature to investigate its electrochemical properties in the anodic region (Fig. 11). Two irreversible oxidation waves are displayed at 0.5 V and 0.85 V (vs $Cp_2Fe^{+/0}$). The first irreversible oxidation can be tentatively identified as a $Pt^{II/III}$process.[49] Generally, the chemical redox chiroptical switches always present reversible oxidation waves in the anodic region.[1] Therefore, the unsuccessful chemical reduction of above-mentioned Pt(IV) complexes is reasonable.

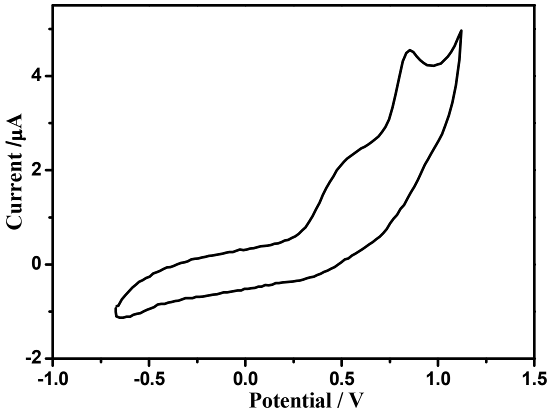

Fig. 11. Cyclic voltammogram of **1a** (10^{-3}M) recorded in CH_2Cl_2 at room temperature (potential vs $Cp_2Fe^{+/0}$).

4. Conclusions

A couple of unprecedented platinum(IV) complexes (**2a** and **2b**) incorporating three phenylacetylene moieties have been facilely obtained by oxidation of cyclometalated platinum(II) complexes **1a** and **1b** at room temperature. Moreover, complexes **1a** and **1b** can be oxidized with an excess of common oxidants (H_2O_2, NaClO, etc.), and the oxidation process is controlled by kinetics. For the solution of complexes **1a** and **1b** before and after oxidation, significantly different absorption, emission as well as chiroptical properties are present due to different coordination configurations. Therefore, we believe that complexes **1a** and **1b** can be used as a candidate of redox responsive materials. Their interesting potential applications will be explored in the future and reported in due course.

Acknowledgements

The authors gratefully acknowledge generous support provided by the National Natural Science Foundation of P.R. China (No.51378253), the Natural Science Foundation of Jiangsu Province (BK20151377), and the Discipline Crossing Foundation of Nanjing University.

Notes and references

1 J. W. Canary, *Chem. Soc. Rev.*, 2009, **38**, 747-756.
2 T. Suzuki, K. Wada, Y. Ishigaki, Y. Yoshimoto, E. Ohta, H. Kawai and K. Fujiwara, *Chem. Commun.*, 2010, **46**, 4100-4102.
3 Z. Dai, J. Lee and W. Zhang, *Molecules*, 2012, **17**, 1247-1277.
4 Y. Le Gal, A. Vacher, V. Dorcet, M. Fourmigué, J. Crassous and D. Lorcy, *New J. Chem.*, 2015, **39**, 122-129.
5 S. Zahn and J.W. Canary, *Science*, 2000, **288**, 1404-1407.
6 A. Iordache, M. Oltean, A. Milet, F. Thomas, B. Baptiste, E. Saint-Aman and C. Bucher, *J. Am. Chem. Soc.*, 2012, **134**, 2653-2671.
7 N. Menard, Y. Heriot, Y. Le Mest, O. Reinaud, N. Le Poul and B. Colasson, *Chem. Eur. J.*, 2013, **19**, 10611-10618.
8 L. Pospisil, L. Bednarova, P. Stepanek, P. Slavicek, J. Vavra, M. Hromadova, H. Dlouha, J. Tarabek and F. Teply, *J. Am. Chem. Soc.*, 2014, **136**, 10826-10829.
9 C. Simão, M. Mas-Torrent, N. Crivillers, V. Lloveras, J. M. Artés, P. Gorostiza, J. Veciana and C. Rovira, *Nat. Chem.*, 2011, **3**, 359-364.
10 Y. Si, G. Yang and Z. Su, *J. Mater. Chem. C*, 2013, **1**, 1399-1406.
11 M. Albrecht, M. Lutz, A. L. Spek and G. van Koten, *Nature*, 2000, **406**, 970-974.
12 S. C. F. Kui, S. S. Y. Chui, C. M. Che and N. Y. Zhu, *J. Am. Chem. Soc.*, 2006, **128**, 8297-8309.
13 J. Ni, X. Zhang, Y.-H. Wu, L.-Y. Zhang and Z.-N. Chen, *Chem. Eur. J.*, 2011, **17**, 1171-1183.
14 O. S. Wenger, *Chem. Rev.*, 2013, **113**, 3686-3733.
15 Y. Sagara and T. Kato, *Nat. Chem.*, 2009, **1**, 605-610.
16 X. Zhang, Z. Chi, Y. Zhang, S. Liu and J. Xu, *J. Mater. Chem. C*, 2013, **1**, 3376-3390.
17 A. Han, P. Du, Z. Sun, H. Wu, H. Jia, R. Zhang, Z. Liang, R. Cao and R. Eisenberg, *Inorg. Chem.*, 2014, **53**, 3338-3344.
18 M. Krikorian, S. Liu and T. M. Swager, *J. Am. Chem. Soc.*, 2014, **136**, 2952-2955.
19 Z. Xue, D. Kuzuhara, S. Ikeda, T. Okujima, S. Mori, H. Uno and H. Yamada, *Inorg. Chem.*, 2013, **52**, 1688-1690.
20 K. M. C. Wong and V. W. W. Yam, *Acc. Chem. Res.*, 2011, **44**, 424-434.
21 X.-D. Wang, O. S. Wolfbeis and R. J. Meier, *Chem. Soc. Rev.*, 2013, **42**, 7834-7869.
22 S. Poirier, R. J. Roberts, D. Le, D. B. Leznoff and C. Reber, *Inorg. Chem.*, 2015, **54**, 3728-3735.
23 R. A. Periana, D. J. Taube, S. Gamble, H. Taube, T. Satoh and H. Fujii, *Science*, 1998, **280**, 560-564.
24 S. M. Drew, D. E. Janzen, C. E. Buss, D. I. MacEwan, K. M. Dublin and K. R. Mann, *J. Am. Chem. Soc.*, 2001, **123**, 8414-8415.
25 A. Kobayashi and M. Kato, *Eur. J. Inorg. Chem.*, 2014, 4469-4483.
26 S. Jamali, S. M. Nabavizadeh and M. Rashidi, *Inorg. Chem.*, 2008, **47**, 5441-5452.
27 R. A. Taylor, D. J. Law, G. J. Sunley, A. J. P. White and G. J. P. Britovsek, *Chem. Commun.*, 2008, 2800-2802.
28 M. Á. Medrano, A. Álvarez-Valdés, J. Perles, J. Lloret-Fillol, S. Muñoz-Galván, A. Carnero, C. Navarro-Ranninger and A. G. Quiroga, *Chem. Commun.*, 2013, **49**, 4806-4808.
29 G. Pelosi, M. Ravera, E. Gabano, F. Fregonese and D. Osella, *Chem. Commun.*, 2015, **51**, 8051-8053.
30 E. Anger, M. Rudolph, L. Norel, S. Zrig, C. Shen, N. Vanthuyne, L. Toupet, J. A. G. Williams, C. Roussel, J. Autschbach, J. Crassous and R. Reau, *Chem. Eur. J.*, 2011, **17**, 14178-14198.
31 E. Anger, M. Rudolph, C. Shen, N. Vanthuyne, L. Toupet, C. Roussel, J. Autschbach, J. Crassous and R. Reau, *J. Am. Chem. Soc.*, 2011, **133**, 3800-3803.
32 T. Wu, X. P. Zhang, C. H. Li, P. Bour, Y. Z. Li and X. Z. You, *Chirality*, 2012, **24**, 451-458.
33 X. P. Zhang, T. Wu, J. Liu, J. C. Zhao, C. H. Li and X. Z. You, *Chirality*, 2013, **25**, 384-392.
34 X.-P. Zhang, J.-F. Mei, J.-C. Lai, C.-H. Li and X.-Z. You, *J. Mater. Chem. C*, 2015, **3**, 2350-2357.
35 X.-P. Zhang, T. Wu, J. Liu, J.-X. Zhang, C.-H. Li and X.-Z. You, *J. Mater. Chem. C*, 2014, **2**, 184-194.
36 M. Hissler, J. E. McGarrah, W. B. Connick, D. K. Geiger, S. D. Cummings and R. Eisenberg, *Coord. Chem. Rev.*, 2000, **208**, 115-137.
37 D. Ravindranathan, D. A. K. Vezzu, L. Bartolotti, P. D. Boyle and S. Huo, *Inorg. Chem.*, 2010, **49**, 8922-8928.
38 U. Knof and A. von Zelewsky, *Angew. Chem. Int. Ed.*, 1999, **38**, 302-322.
39 X.-P. Zhang, V. Y. Chang, J. Liu, X.-L. Yang, W. Huang, Y. Li, C.-H. Li, G. Muller and X.-Z. You, *Inorg. Chem.*, 2015, **54**, 143-152.

40 *SAINT-Plus*, version 6.02, Bruker Analytical X-ray System: Madison, WI, 1999.

41 G. M. Sheldrick, *SADABS*, an empirical absorption correction program,Bruker Analytical X-ray Systems: Madison, WI, 1996.

42 G. M. Sheldrick, *ActaCryst.*, 2008, A**64**, 112-122.

43 Gaussian 03, Revision E.01, M. J. Frisch, G. W. Trucks, H. B. Schlegel,G. E. Scuseria, M. A. Robb, J. R. Cheeseman, J. A. Montgomery, Jr., T. Vreven, K. N. Kudin, J. C. Burant, J. M. Millam, S. S. Iyengar, J. Tomasi, V. Barone, B. Mennucci, M. Cossi, G. Scalmani, N. Rega, G. A. Petersson, H. Nakatsuji, M. Hada, M. Ehara, K. Toyota, R. Fukuda, J. Hasegawa, M. Ishida, T. Nakajima, Y. Honda, O. Kitao, H. Nakai, M. Klene, X. Li, J. E. Knox, H. P. Hratchian, J. B. Cross, V. Bakken, C. Adamo, J. Jaramillo, R. Gomperts, R. E. Stratmann, O. Yazyev, A. J. Austin, R. Cammi, C. Pomelli, J. W. Ochterski, P. Y. Ayala, K. Morokuma, G. A. Voth, P. Salvador, J. J. Dannenberg, V. G. Zakrzewski, S. Dapprich, A. D. Daniels, M. C. Strain, O. Farkas, D. K. Malick, A. D. Rabuck, K. Raghavachari, J. B. Foresman, J. V. Ortiz, Q. Cui, A. G. Baboul, S. Clifford, J. Cioslowski, B. B. Stefanov, G. Liu, A. Liashenko, P. Piskorz, I. Komaromi, R. L. Martin, D. J. Fox, T. Keith, M. A. Al-Laham, C. Y. Peng, A. Nanayakkara, M. Challacombe, P. M. W. Gill, B. Johnson, W. Chen, M. W. Wong, C. Gonzalez and J. A. Pople, Gaussian, Inc., Wallingford CT, 2004.

44 D. Andrae, U. Haeussermann, M. Dolg, H. Stoll and H. Preuss, *Theor. Chim. Acta*, 1990, **77**, 123-141.

45 F. P. Fanizzi, G. Natile, M. Lanfranchi, A. Tiripicchio, F. Laschi and P. Zanello, *Inorg. Chem.*, 1996, **35**, 3173-3182.

46 G. D. Batema, M. Lutz, A. L. Spek, C. A. van Walree, C. d. M. Donega, A. Meijerink, R. W. A. Havenith, J. Perez-Moreno, K. Clays, M. Buechel, A. van Dijken, D. L. Bryce, G. P. M. van Klink and G. van Koten, *Organometallics*, 2008, **27**, 1690-1701.

47 K. R. Pellarin, M. S. McCready, T. I. Sutherland and R. J. Puddephatt, *Organometallics*, 2012, **31**, 8291-8300.

48 B. N. Ghosh, D. Lentz and S. Schlecht, *New J. Chem.*, 2015, **39**, 3536-3542.

49 W. Lu, B. X. Mi, M. C. W. Chan, Z. Hui, C. M. Che, N. Y. Zhu and S. T. Lee, *J. Am. Chem. Soc.*, 2004, **126**, 4958-4971.

50 J. Schneider, P. Du, P. Jarosz, T. Lazarides, X. Wang, W. W. Brennessel and R. Eisenberg, *Inorg. Chem.*, 2009, **48**, 4306-4316.

51 X.-N. Li, Z.-J. Wu, L. Zhou, X.-J. Liu and H.-J. Zhang, *Org. Electron.*, 2011, **12**, 51-61.

52 B. Zhang, Y. Li, R. Liu, T. M. Pritchett, A. Azenkeng, A. Ugrinov, J. E. Haley, Z. Li, M. R. Hoffmann and W. Sun, *Chem. Eur. J.*, 2012, **18**, 4593-4606.

53 C. Latouche, P.-H. Lanoe, J. A. G. Williams, V. Guerchais, A. Boucekkine and J.-L. Fillaut, *New J. Chem.*, 2011, **35**, 2196-2202.

54 X. Zhou, Q. J. Pan, B. H. Xia, M. X. Li, H. X. Zhang and A. C. Tung, *J. Phys. Chem. A*, 2007, **111**, 5465-5472.

55 M. La Deda, A. Crispini, I. Aiello, M. Ghedini, M. Amati, S. Belviso and F. Lelj, *Dalton Trans.*, 2011, **40**, 5259-5270.

56 Y. Shimazaki, T. Yajima, F. Tani, S. Karasawa, K. Fukui, Y. Naruta and O. Yamauchi, *J. Am. Chem. Soc.*, 2007, **129**, 2559-2568.

57 K. Uemura, T. Kanbara and M. Ebihara, *Inorg. Chem.*, 2014, **53**, 4621–4628.

58 J. E. Sarneski, A. T. McPhail, K. D. Onan, L. E. Erickson and C. N. Reilley, *J. Am. Chem. Soc.*, 1977, **99**, 7376-7378.

59 C. Kolbeck, N. Taccardi, N. Paape, P. S. Schulz, P. Wasserscheid, H.-P. Steinrück and F. Maier, *J. Mol. Liq.*, 2014, **192**, 103-113.

60 N. Komiya, T. Muraoka, M. Iida, M. Miyanaga, K. Takahashi and T. Naota, *J. Am. Chem. Soc.*, 2011, **133**, 16054-16061.

61 T. Tu, W. Fang, X. Bao, X. Li and K. H. Doetz, *Angew. Chem. Int. Ed.*, 2011, **50**, 6601-6605.

62 K. Liu, L. Meng, S. Mo, M. Zhang, Y. Mao, X. Cao, C. Huang and T. Yi, *J. Mater. Chem. C*, 2013, **1**, 1753-1762.

63 N. Saleh, B. MooreII, M. Srebro, N. Vanthuyne, L. Toupet, J. A. G. Williams, C. Roussel, K. K. Deol, G. Muller, J. Autschbach and J. Crassous, *Chem. Eur. J.*, 2015, **21**, 1673-1681.

64 M. Sinisi, F. P. Intini and G. Natile, *Inorg. Chem.*, 2012, **51**, 9694-9704.

Journal Name

ARTICLE

Graphical Abstract

A couple of unprecedented platinum(IV) complexes have been facilely prepard, and distinct chiroptical performances are exhibited.